Vaccine 56 (2025) 127183

Contents lists available at ScienceDirect

Vaccine

journal homepage: www.elsevier.com/locate/vaccine

Mucosal vaccines with STING-agonist liposomal formulations inhibit RSV (respiratory syncytial virus) replication in cotton rats

K M Samiur Rahman Sefat [a], Rohan Kulkarni [a], Jason Trinh [a], Ankita Leekha [a], Monish Kumar [a], Haoran Wu [b], Trevor McBride [c], Letisha Aideyan [c], Vasanthi Avadhanula [c], Pedro A. Piedra [c], Stacey M. Louie [b], Navin Varadarajan [a,*]

[a] Department of Chemical and Biomolecular Engineering, University of Houston, Houston, TX 77204, United States
[b] Department of Civil & Environmental Engineering, University of Houston, Houston, TX 77204, United States
[c] Department of Molecular Virology and Microbiology, Baylor College of Medicine, Houston, TX 77030, United States

ARTICLE INFO

Keywords:
Vaccine
RSV
NanoSTING
Liposomes
Intranasal

ABSTRACT

Respiratory syncytial virus (RSV) is responsible for severe lower respiratory tract infections (LRTI) in immunocompromised individuals. While recent breakthroughs in vaccine design have led to approved vaccines for the elderly, these vaccines are all administered through the parenteral route. Vaccine administration through the mucosal route could protect the viral route of entry and can be advantageous over injected vaccines. There is however a lack of safe and efficacious mucosal adjuvants that can facilitate both mucosal and systemic immune responses. Here, we present preclinical data based on liposomal nanoparticles, NanoSTING, that encapsulate the endogenous STING-agonist 2′3′-cGAMP (cyclic guanosine adenosine monophosphate) as adjuvant for prefusion protein-based intranasal vaccines against RSV. NanoSTING significantly increased the immunogenicity of well-documented RSV prefusion protein antigens DS-CaV1, sc9-10 DS-CaV1, and SC-TM after a single intranasal dose, when compared to the protein-only and naked-cGAMP adjuvanted groups. Two doses of NanoSTING adjuvanted vaccines yielded robust secretory IgA titers at the mucosal surfaces and induced potent Th1 T-cell responses in the lungs of vaccinated mice. Both NanoSTING-sc9-10 DS-CaV1 and NanoSTING-SCTM vaccines protect against viral replication at the upper (nose) and lower (lung) respiratory tract of RSV-challenged cotton rats. The ability of our mucosal vaccines against RSV to elicit immunity in the respiratory tract can prevent the establishment of infection in individuals and potentially prevent disease transmission.

1. Introduction

Human respiratory syncytial virus is a highly infectious, ubiquitous virus responsible for severe respiratory tract disease in children and the elderly [1]. About one-third of deaths resulting from acute lower respiratory infection (ALRI) are caused by the virus in the first year of life [2], and nearly all children have been infected by RSV at least once by 24 months of age [3]. A recent study estimated that, in 2019, there were 33 million RSV-associated lower respiratory tract (LRT) infections and 101,400 RSV-related deaths worldwide in children under 5 years of age [4]. RSV infection is also a leading cause of disease among adults older than 65 years, with approximately 177,000 hospitalizations and 14,000 deaths each year in the United States [5]. Effective vaccination against RSV can help relieve the tremendous burden of RSV on infants and older individuals.

After the initial failures with the formalin-inactivated RSV vaccine, protein-based vaccines have been prioritized due to their well-documented history of safety. The RSV virion presents three proteins on the viral membrane that can be targeted for vaccine development: small-hydrophobic protein (SH), attachment protein (G), and fusion protein (F). The SH protein is important for viral replication *in vivo* [6,7], and helps the virus evade host immune response [8]. SH protein elicits binding antibodies that cannot neutralize the virus; however, these antibodies can protect RSV-challenged mice against viral replication *via* the Fc-mediated ADCC (antibody-mediated cellular cytotoxicity) pathway [9,10].

The RSV F protein is highly conserved among the virus subtypes [11] and have been safely tested in clinical trials that led to the approval of

* Corresponding author.
E-mail address: nvaradar@central.uh.edu (N. Varadarajan).

https://doi.org/10.1016/j.vaccine.2025.127183
Received 8 January 2025; Received in revised form 23 April 2025; Accepted 23 April 2025
Available online 2 May 2025

two fusion protein-based vaccines for people over the age of 65. The 574 amino acid protein is composed of two subunits (F1 and F2) linked together by disulfide bonds [12]. Three such protomers then assemble on the viral membrane to form the trimeric fusion protein [13]. The native fusion protein is metastable and spontaneously refolds into the postfusion form. Six antibody-neutralizing epitopes have been discovered on the fusion protein (I, II, III, IV, V, and Φ) [14]. Most potent neutralizing antibodies are directed against epitope Φ, which is only present on the prefusion protein [14].

The development of protective RSV-F vaccines based on the prefusion F protein has been guided extensively by structure-based antigen design. Three prefusion F-specific neutralizing antibodies—D25 [15], AM22 [16], and 5C4 [17]— were instrumental in determining the structure of the prefusion RSV-F, which paved the way for the design of the first prefusion-stabilized F protein with an additional interprotomer disulfide bond and cavity-filling substitutions, DS-Cav1 [18]. This success was followed by iterative cycles of structure-based design, resulting in second-generation immunogens, which substantially enhanced the titer of RSV-protective immune responses [19]. Optimization of flexible glycine-serine (GS) linker length between the F1 and F2 subunits improved upon the stability of DS-CaV1 and resulted in genetically linked F-subunit designs like sc9-10 DS-CaV1 [19]. Independently, a structure-based design was used to identify SC-TM that incorporated novel stabilizing mutations to yield high expression levels while maintaining a stable prefusion conformation [20]. This design stabilized the protein in its prefusion form by engineering mutations N67I, S215P, and E487Q to restrict the movement of the secondary structural elements that rearrange during the transformation from prefusion to postfusion conformation. Although these diverse designs have been reported to stabilize prefusion RSV-F, a direct comparison of these antigens in the context of mucosal vaccines has not been reported.

Mucosal immunity induced by respiratory viruses, including RSV, is increasingly recognized as a decisive factor in disease outcomes following reinfections [21,22]. Antigen-specific secretory IgA lining the nasal mucosa is the first layer of protection against reinfection, and levels of mucosal IgA were shown to be correlated with protection from disease caused by RSV in adults [23]. RSV vaccines in the clinic are all administered intramuscularly, and even though repeated parenteral vaccinations could lead to modest levels of mucosal IgA in the respiratory tract, mucosal vaccines are more efficient in this regard [24]. Despite their appeal, developing a mucosal vaccine against RSV has been challenging due to a lack of safe and potent adjuvants for RSV fusion protein immunogens.

Here, we encapsulated the STING-agonist 2′3′-cGAMP inside negatively charged lipid-based liposomes to formulate a nanoparticle adjuvant efficient at priming the mucosal immunity for an effective immune response [25]. We utilized the DS-CaV1, sc9-10 DS-CaV1 (sc9-10) and SCTM prefusion protein designs as immunogens in our vaccine and report that NanoSTING adjuvanted vaccines induce robust humoral and cellular immunity against RSV, resulting in protection from viral replication in the respiratory tract. Our data indicates that NanoSTING enhances the immunogenicity of established protein antigens and could be adopted as an adjuvant platform for developing mucosal vaccines.

2. Materials and methods

2.1. Expression and purification prefusion proteins

We ordered the DS-CaV1 plasmid construct from Genscript (NJ, USA) based on the amino acid sequence published by McLellan et al. [11], and the sc9-10 DS-CaV1 plasmid was a generous gift from Dr. Peter Kwong (NIH, Bethesda, MD). The SCTM protein-expressing plasmid was obtained from Janssen Pharmaceuticals (Beerse, Belgium). We used the Expi293™ expression system (Thermo Scientific, MA, USA) to express all the protein variants. We cultured Expi293™ cells in a shaking incubator at 37 °C and 8 % CO_2, according to manufacturer recommendations, until the desired cell density of 3–5 × 10^6 cells/mL was obtained. Plasmid DNA encoding the prefusion proteins was transiently transfected into the cells using the ExpiFectamine™ 293 transfection kit. We collected the culture supernatants containing the expressed RSV fusion proteins five days after the transfection by centrifuging the cell suspension at 5000 ×g for 20 mins. The supernatant was sterile-filtered using a 0.22 μm filter and stored at −80 °C until further use.

We purified the 6 × his tagged DS-CaV1 and sc9-10 DS-CaV1 proteins using a two-step purification protocol applying immobilized metal affinity (IMAC) and size-exclusion chromatography (SEC) on an ÄKTA™ UV-900, P-900, pH/C-900, Frac-950 purification system (GE healthcare life sciences, IL, USA). For affinity chromatography, nine volumes of harvested supernatant were mixed with one volume of 10 × loading buffer (50 mM NaH_2PO_4, 300 mM NaCl, 10 mM Imidazole, and 0.01 % Tween20, pH = 8.0). The supernatant was passed over an XK 16/20 column packed with 5 mL Ni Sepharose 6 Fast Flow to load the protein on the resin. Then we washed the column with 10 CV (column volume) of wash buffer (50 mM NaH_2PO_4, 300 mM NaCl, 20 mM Imidazole, and 0.01 % Tween-20, pH = 8.0) and eluted the protein with 2 CV elution buffer (50 mM NaH_2PO_4, 300 mM NaCl, 250 mM Imidazole and 0.01 % Tween-20, pH = 8.0). The eluted fractions were promptly exchanged into PBS using a 3 kDa molecular weight cut-off Slide-A-Lyzer dialysis cassette (ThermoFisher Scientific, MA, USA). We concentrated the eluted fractions and purified them on a Superdex-200 (GE Healthcare Life Sciences, IL, USA) SEC column using PBS as a running buffer.

The SCTM protein was purified using a combination of ion exchange chromatography (IEX) and SEC steps. We diluted the culture supernatant with two volumes of 50 mM NaOAc, pH = 5.0, and loaded the protein on a 5 mL SP Sepharose cation exchange resin (Cytiva, MA, USA). We washed the column with 10 CV of wash buffer (20 mM NaOAc, 50 mM NaCl, 0.01 % Tween20, pH = 5.0) and eluted the protein using a linear gradient of NaCl from 100 mM to 1 M. We concentrated the eluate and purified it further using SEC, following similar steps as for DS-CaV1 and sc9-10 DS-CaV1.

2.2. NanoSTING preparation

We prepared cGAMP-encapsulating nanoparticles as described previously [26]. Briefly, we prepared a 10:1:1:1 M mixture of DPPC, DPPG, Cholesterol (Chol), and DPPE-PEG2000 (Avanti Polar Lipids, AL, USA) in $CHCl_3$ and CH_3OH. The solvent was evaporated using a vacuum rotary evaporator at 45 °C until a thin lipid film was observed. We added prewarmed cGAMP (Medchem Express, NJ, USA) solution (1.5 mg/mL in PBS) to hydrate the film and sonicated the mixture for 60 min. The mixture was further subjected to five freeze-thaw cycles, and membrane extrusion through a 200 nm membrane (Cytiva, MA, USA, Cat #10417004) to generate particles of uniform size. Free, unencapsulated cGAMP was removed from the resulting nanoparticles using Amicon ultrafiltration units (10 kDa MW cutoff). We utilized an HPLC method to evaluate the encapsulation efficiency of cGAMP by generating a standard curve with cGAMP solutions ranging from 0.01 mg/mL to 0.15 mg/mL, followed by analysis using an HPLC column. To quantify the encapsulated cGAMP, liposomes were disrupted by adding methanol, releasing the cGAMP for analysis by HPLC. The resulting HPLC peak was then compared to the standard curve to determine the encapsulated cGAMP content.

2.3. Western blot analysis

We analyzed the expressed and purified proteins by electrophoresing through 4–15 % Mini-PROTEAN TGX (BioRad, CA, USA) gels under reducing and denaturing conditions. We added 2-mercaptoethanol (Sigma Life Science, Burlington, MA) to the protein samples to disrupt the disulfide bonds and incubated the samples at 95 °C for 5 min to denature the protein. Vertical electrophoresis was performed with 1 ×

tris/glycine/SDS running buffer for 2 h at 90 V. Immediately after the electrophoresis, the protein was blotted on a polyvinylidene fluoride (PVDF) membrane using 1× tris/glycine/methanol transfer buffer for 1 h at 90 V. We incubated the membrane in 1× tris-buffered saline/Tween20 (TBST) (J.T. Baker/Fisher Bioreagents; PA, USA; Sigma, MO, USA) containing 5 % skim milk to block active binding sites of the protein. Following 2 h of blocking, we incubated the membranes overnight in the primary antibody solution of 2.5 % bovine serum albumin (BSA) (ThermoFisher Scientific, MA, USA) in TBST. The primary antibodies used for the detection of RSV fusion proteins were the anti-RSV antibody MAB8599 (MilliporeSigma, MA, USA) and the anti-his tag antibody (Clone: J095G46) (BioLegend, CA, USA). We incubated the membrane overnight with an anti-mouse IgG HRP (Cell Signalling Technology, MA, USA) secondary antibody for 1 h. Finally, the membranes were washed three times with TBST buffer and developed using Pierce 1-Step Ultra TMB Blotting Solution (ThermoFisher Scientific) as per manufacturer recommendations. Images were taken using cell phone cameras and analyzed using ImageJ software.

2.4. SEC-MALS

The molar mass of the RSV F proteins was determined by SEC-MALS analysis. The protein samples were filtered using a 0.22 μm nylon syringe filter (MicroSolv, Wilmington, NC) prior to analysis. Separation was achieved on a Superdex 200 Increase 10/300 GL SEC column (GE Healthcare, Chicago, IL) for 100 μL sample injection volumes (Agilent 1290 Infinity autosampler, Agilent Technologies Santa Clara, CA). The mobile phase was 0.22 μm-filtered phosphate-buffered saline (PBS) at a flow rate of 0.5 mL/min (Agilent 1290 Infinity binary pump). Concentration detection of the eluting protein was provided by an Agilent 1260 Infinity UV–vis diode array detector at 280 nm wavelength using a UV extinction coefficient of 0.95 mL mg^{-1} cm^{-1} [25] for RSV F protein. Light scattering data were collected on a Wyatt HELEOS II MALS detector (Wyatt Technologies, Santa Barbara, CA), using a 1st-order Zimm analysis as implemented in the Wyatt ASTRA 7.3.2 software for molar mass determination. Detector alignment, band broadening corrections, and normalization of the MALS detectors across the various scattering angles were performed using a sample of bovine serum albumin (BSA) at 1 g/L, which was run before the RSV F analyses. It is noted that a Wyatt OptiLab T-rEX differential refractive index (dRI) detector was also used and yielded consistent molar mass results to the UV–vis detector for a refractive index increment (dn/dc) of 0.185 mL/g for the protein.

2.5. Mouse studies

We performed all mouse experiments in accordance with the guidelines provided by the Institutional Animal Care and Use Committee (IACUC). We purchased six- to ten-week-old female Balb/c mice from The Jackson Laboratory (ME, USA). We housed them at the institutional animal facility of the University of Houston for at least 10 days before the start of the experiments. The animals were vaccinated intranasally using these vaccine formulations: 1) PBS, 2) 10 μg DS-CaV1, 3) 10 μg DS-CaV1 + 20 μg NanoSTING, 4) 10 μg SCTM +20 μg cGAMP, 5) 10 μg SCTM +20 μg NanoSTING, 6) 10 μg sc9-10 DS-CaV1 + 20 μg NanoSTING. Mice were anesthetized with isoflurane prior to intranasal vaccine administration. The vaccine was delivered at a volume of 10–15 μL per nostril, resulting in a total administered volume of 20–30 μL per mouse. Three weeks after the first dose, the mice were boosted with the corresponding prime dosage. Mice were bled every week to record antibody response. All animals were euthanized five weeks after the first vaccination, and tissue (lung and spleen) samples were collected for ELISpot.

2.6. Nasal wash and Bronchoalveolar lavage fluid (BALF) collection

To collect the nasal wash, we made a small incision in the mouse trachea and inserted a 23 g catheter. Using a 3 mL syringe, we injected 1–1.5 mL sterile PBS + 0.05 % BSA solution through the nose and collected the nasal wash by placing a 1.5 mL microcentrifuge tube under the nasal opening of the mice. Bronchoalveolar lavage (BAL) was performed by inserting a catheter into the trachea of terminally anesthetized mice. We gently injected 3 mL PBS + 0.05 % BSA in the lung and aspirated the solution. Both nasal wash and BALF solutions were centrifuged at 800*g* for 15 min at 4 °C to remove cells. We collected the supernatants carefully and added a protease inhibitor cocktail (Roche, CH) and PMSF (ThermoFisher, MA, USA) before storing the solutions at −80 °C until later use.

2.7. ELISA

Using ELISA, we tested the magnitude of vaccine-induced antibody response in serum against the fusion proteins. In short, we incubated high protein binding ELISA plates (Corning, NY, USA) with RSV prefusion proteins at 0.5 μg/mL in phosphate-buffered saline (PBS) overnight at 4 °C or 2 h at 37 °C. We washed the plates with PBS + 0.05 % Tween20 (PBST) to remove unbound protein. The plates were blocked with PBS + 1 % BSA (Fisher Scientific, PA, USA) + 0.1 % Tween20 for 2 h at room temperature. Following three more washes with PBST, we added the serum samples at different dilutions to the plate. To detect RSV prefusion binding antibodies, we washed the plates with PBST and added HRP-conjugated anti-mouse IgG (Jackson ImmunoResearch Laboratories, 1:6000; PA, USA) or Biotin-conjugated Goat anti-mouse IgA (Southern Biotech, 1:5000; AL, USA). Streptavidin-HRP (Vector Laboratories, 1:2500, CA, USA) detected an anti-IgA secondary antibody. Finally, we developed the plates using 1-Step™ TMB ELISA substrate (ThermoFisher Scientific).

2.8. Lung lymphocyte and splenocyte collection

We harvested lung and spleen cells from vaccinated mice to test antigen-specific T-cell responses. In short, we perfused the lung vasculature with 5 mL of 0.1 mM EDTA in PBS without Ca^{2+} or Mg^{2+}, injecting it into the right cardiac ventricle to remove red blood cells (RBCs). Each lung was cut into 100–300 mm^2 pieces and transferred into a digestion buffer containing collagenase D (2 mg/mL, Roche) and DNase (0.125 mg/mL, Sigma) in 5 mL RPMI. The tissue was incubated at 37 °C for 1.5 h, vortexing every 10 min. The remaining intact tissue was disrupted by passing it through a 21-gauge needle 6–8 times. The reaction was stopped by adding 500 μL of ice-cold buffer (1× PBS, 0.1 M EDTA). The suspension was passed through a 40 μm cell strainer (Falcon), and single cells were collected in a 50 mL tube. Cells were centrifuged at 600 x*g* for 10 min to form a pellet. The remaining RBCs were lysed using 3 mL of ACK Lysing Buffer (Invitrogen), followed by another centrifugation at 600 x*g* for 10 min. The pellet was resuspended in 5 mL RPMI media (Corning). Spleens were stored in RPMI medium until processed, then homogenized by passing through a 40 μm strainer. RBCs were removed by incubating splenocytes in 3 mL ACK lysis solution for 3 min at room temperature, and the mixture was passed through a 40 μm strainer. Trypan blue exclusion was used to count splenocytes and lung cells.

2.9. ELISpot

To perform the ELISpot assays, we incubated plates (Ref: MSIPS4W10, Millipore, MA, USA) with anti-IFNγ antibody (1 μg/mL, Ref: 3321–3-250, Mabtech, VA, USA) at 4 °C overnight. We washed the plates with sterile PBS five times the next day and added lung lymphocytes and splenocytes. We treated the cells from mice with 1) R10 media (negative control), 2) 12-myristate 13-acetate (PMA) (Sigma, St. Louis, MI, USA), and 1 μg/mL of ionomycin (positive control), and 3) RSV fusion protein peptide pool (2 μg/mL/peptide, JPT, Germany). For positive control, 1×10^4 cells were stimulated in triplicates, whereas we

stimulated 3 × 10^5 cells in the rest of the wells. Following overnight stimulation of the cells, we washed the plates with PBS and added a biotinylated anti-IFNγ (1 μg/mL, Ref: 3321-6-250, Mabtech) detection antibody. After 1 h of incubation at 37 °C, we rewashed the plates and added diluted Extravidin-ALP conjugate (1:30,000, Sigma, St. Louis, MI, USA). Finally, the spots were developed by adding BCIP/NBT-plus substrate (Ref: 3650–10, Mabtech). We rinsed off the substrate with water and imaged the spots using Cytation 7 (BioTek Instruments, Inc.) imaging plate reader. The spots were enumerated using Gen5 (BioTek) software.

2.10. Virus

Respiratory Syncytial Virus strain A/A2 (RSV A/A2) (ATCC, Manassas, VA) was propagated in HEp-2 cells after serial plaque-purification to reduce defective-interfering particles. A pool of virus designated as hRSV A/A2 Lot# 092215 SSM containing approximately 3.0 × 10^8 pfu/mL in sucrose stabilizing media (25 % of Sucrose in PBS) was used in this *in vivo* experiment. Virus stock was stored at −80 °C and has been characterized *in vivo* using the cotton rat model and validated for upper and lower respiratory tract replication.

2.11. Cotton rat studies

Twenty-five (25) inbred, 5–7 weeks-old, *Sigmodon hispidus* female cotton rats (source: Sigmovir Biosystems, Inc., Rockville, MD) were maintained and handled under veterinary supervision in accordance with the National Institutes of Health guidelines and Sigmovir Institutional Animal Care and Use Committee's approved animal study protocol (IACUC Protocol #15). Cotton rats were housed in clear polycarbonate cages and provided with standard rodent chow (Harlan #7004) and tap water *ad lib.* The cotton rats were intranasally immunized twice (four weeks apart) in groups of 5–8 animals with 1) PBS, 2) 20 μg sc9-10 + 40 μg NanoSTING, 3) 20 μg SCTM+ 40 μg NanoSTING. We anesthetized the animals with isoflurane and administered 30–35 μL of the intranasal vaccine, delivering half the volume into each nostril of the cotton rats. A group of five cotton rats were intramuscularly immunized with FI-RSV as control animals. Three weeks after the booster dose, the animals were challenged with a total of 10^5 plaque-forming units (p.f.u.) of RSV A2 virus in 100 μL volume. The animals were lightly anesthetized with isoflurane before the challenge. Four days after the challenge, we collected the lung and nasal tissues to evaluate viral titers.

2.12. RSV-specific microneutralization assay

Heat-inactivated sera samples were diluted 1:10 with EMEM and serially diluted further 1:4. We incubated the diluted sera samples with RSV A2 (25–50 PFU) for 1 h at 25 °C and inoculated duplicates onto confluent HEp-2 monolayers in 24-well plates. After one hour incubation at 37 °C in a 5 % CO2 incubator, the wells were overlayed with 0.75 % Methylcellulose medium. After 4 days of incubation, the overlay was removed, and the cells were fixed with 0.1 % crystal violet (dissolved in 25 % glutaraldehyde in water solution) stain for one hour and then rinsed and air dried. Serum neutralizing antibody to RSV was assayed by measuring 60 % plaque reduction on Hep-2 cell monolayers [27]. RSV B-specific virus-neutralizing titers were determined using HEp-2 cell monolayers infected with RSV/B/18537. We defined RSV B neutralizing titers as the highest serum dilution at which we observed at least a 50 % reduction in viral replication. We assigned a value of 2 $\log_2$ for any serum sample exhibiting neutralizing titers less than the lower limit of detection (2.5 $\log_2$) [28].

2.13. Lung and nose viral titration

The rostral portion of the nose, including the turbinates, was carefully dissected and homogenized in 3 mL of media. We removed the lungs en bloc and homogenized the left lobe for viral titration. We clarified the lung and nose homogenates by centrifugation at 600 x*g* for 10 min and diluted them in EMEM media. Confluent HEp-2 monolayers were infected in duplicates with diluted homogenates in 24-well plates. After one hour incubation at 37 °C in a 5 % CO_2 incubator, the wells were overlayed with 0.75 % Methylcellulose medium. After 4 days of incubation, we removed the overlays and fixed the cells with a 0.1 % crystal violet stain for one hour. The wells were properly rinsed and air-dried. Plaques were counted, and virus titer was expressed as plaque-forming units per gram of tissue. Viral titers are calculated as geometric mean ± standard error for all animals in a group at a given time.

2.14. Statistical analysis

We presented all data as mean values, and error bars represent ±SEM (standard error of the mean). All statistical analyses were performed using GraphPad Prism (V8). We compared two groups using the Mann-Whitney *t*-test, while comparisons between multiple groups were performed using Tukey's multiple tests for repeated measures analysis.

3. Results

3.1. Purification, preparation, and characterization of prefusion protein-based vaccines

Most RSV-neutralizing antibodies are directed against the prefusion protein. As per the original publications, the amino acid substitutions that stabilize the prefusion proteins DS-CaV1, sc9-10, and SCTM are annotated in Fig. 1A. We expressed these proteins in an Expi293 suspension-culture expression system (Supplementary Fig. 1A) and verified their expression in the supernatant using anti-RSV F western blot (Fig. 1B).

The molecular weight of the purified proteins was analyzed using SEC-MALS. The SEC chromatogram shows a major peak corresponding to the trimeric protein (Supplementary Fig. 1B). We analyzed the multi-angle light-scattering data, which confirmed the size of the sc9-10 and SCTM trimeric proteins in the expected molecular weight range (~160–180 kDa). Notably, the sc9-10 DS-CaV1 chromatogram also indicates the presence of a minor species corresponding to a 320–400 kDa protein, which could have formed due to the association of two molecules of the trimeric protein. The final yields of the prefusion trimers were determined using an AM14-prefusion protein-specific ELISA (Supplementary Fig. 1C). AM14 is a monoclonal antibody that recognizes an epitope spanning two protomers of the RSV prefusion protein trimer, and previous studies have reported that this antibody does not bind to the monomeric RSV fusion protein [29]. We observed prefusion trimer yields ranging from 1 mg/L for DS-CaV1 to 50 mg/L for SCTM in Expi293 expression system (Supplementary Fig. 1C).

To synthesize the adjuvant, we encapsulated 2′3′-cGAMP in lipid-based nanoparticles (NanoSTING), as described previously [26]. We mixed the purified prefusion proteins with NanoSTING at 25 °C for 15 min in a single-step "mix and immunize" approach to formulate the vaccines for animal studies. We performed dynamic light scattering (DLS) on the nanoparticles before (116 ± 7 nm) and after (121 ± 3 nm) mixing with DS-CaV1, revealing comparable particle sizes (Fig. 1C). The other NanoSTING-adjuvanted vaccine formulations exhibited comparable nanoparticle sizes (not shown). DLS did not indicate any signs of protein aggregation in the vaccines, at least for the duration of immunizations (30 min- 1 h). We proceeded to use these vaccines for *in vivo* studies.

3.2. NanoSTING adjuvanted vaccines improve immunogenicity of RSV prefusion proteins in mice

We evaluated the immunogenicity of NanoSTING adjuvanted

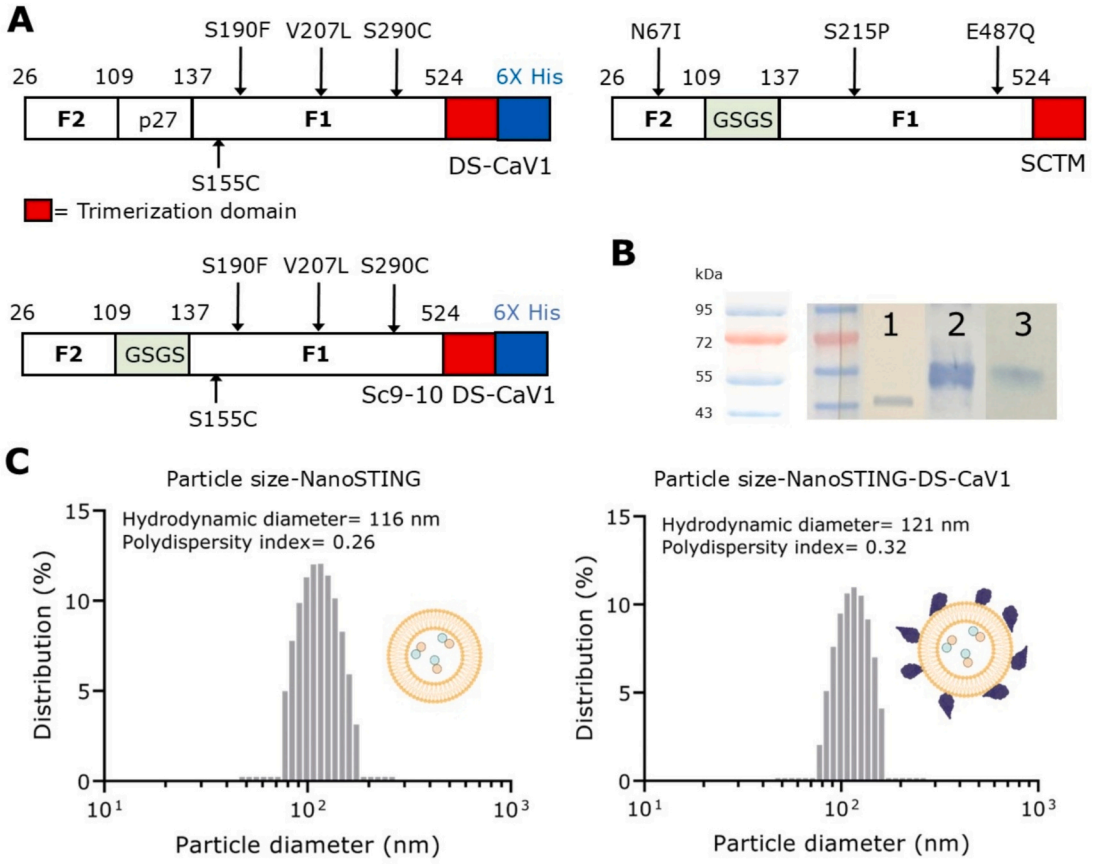

Fig. 1. Expression and characterization of RSV fusion protein-based vaccine.
A) Construct design for RSV fusion protein variants DS-CaV1, sc9-10 and SCTM.
B) Anti-RSV-F Western blot of cell culture supernatant electrophoresed in a denaturing gel. Lane 1: DS-CaV1 (45 kDa), Lane 2: SCTM (55 kDa), Lane 3: sc9-10 (55 kDa).
C) Distribution of liposomal particle sizes in NanoSTING and NanoSTING-DS-CaV1 by dynamic light scattering (DLS).

intranasal vaccines in mice. Groups of Balb/c mice were immunized with a single dose of: 1) PBS, 2) DS-CaV1 (no adjuvant), 3) NanoSTING-DS-CaV1, 4) cGAMP-SCTM (no liposomes), 5) NanoSTING-SCTM, and 6) NanoSTING-sc9-10 vaccines. Prefusion protein-specific antibody titers increased from day 7 to day 21 for all the groups and were no different when comparing the three antigens immunized with NanoSTING as an adjuvant (Fig. 2B). Notably, serum IgG titers were significantly lower (p-value = 0.006) in the unadjuvanted DS-CaV1 immunized ($4 \pm 1 \times 10^2$) group compared to NanoSTING-DS-CaV1 ($6 \pm 2 \times 10^3$). Additionally, naked 2′3′-cGAMP adjuvanted SCTM immunized mice also exhibited much lower prefusion protein specific titers ($1.5 \pm 0.6 \times 10^3$, p-value = 0.04) compared to NanoSTING-SCTM ($5 \pm 1 \times 10^3$). To evaluate the durability of vaccine-induced immunity, we immunized a group of mice with NanoSTING-DS-CaV1 and tested prefusion protein-specific antibody titers in serum six months after immunization. The serum IgG endpoint titers 180 days post-immunization ($2.6 \times 10^3 \pm 4 \times 10^2$) were comparable to day 21 titers, suggesting durable humoral immunity (Supplementary Fig. 3).

Unlike the serum IgG titers, the serum IgA titers were detectable but modest following a single intranasal dose of the vaccines (Supplementary Fig. 2B). Next, we wanted to test the nature of cellular immunity induced by NanoSTING-adjuvanted vaccines. Extensive studies on failed RSV vaccines have associated vaccine-induced enhanced respiratory disease (ERD) with Th2 response, and a Th1 T-cell response is desirable for safe and protective cellular immunity [30,31]. We performed ELISpot to quantify T-cell responses stimulated by RSV A2 fusion protein peptides. The antigen-specific T-cell responses in the lung/spleen showed a Th1 bias and were detectable but variable across the different antigens adjuvanted with NanoSTING (*e.g.* NanoSTING-DS-CaV1, lung: $8 \pm 2 \times 10^2$, spleen: $6 \pm 1 \times 10^2$)[Supplementary Fig. 2B]. Collectively, these results established that while liposomal NanoSTING is essential for robust serum IgG responses, a single dose vaccine yields only modest mucosal responses that is dependent on the antigen.

To improve the mucosal immune response elicited upon vaccination, we prioritized the NanoSTING-sc9-10 and NanoSTING-SCTM vaccines and utilized a prime-boost vaccination strategy (Fig. 2A). We did not include DS-CaV1 in the prime-boost study and subsequent challenge studies due to low protein expression titers. Following the booster dose, we collected serum from vaccinated animals on day 48 to evaluate the IgG and IgA responses. Prefusion protein-specific serum IgG increased in both NanoSTING-sc9-10 ($1 \pm 0.3 \times 10^5$ on day 48 *vs* $5 \pm 1 \times 10^3$ on day 21) and NanoSTING-SCTM ($1 \pm 0.5 \times 10^5$ on day 48 *vs* $5 \pm 1 \times 10^3$ on day 21) groups following the booster (Fig. 2B). RSV-specific nasal IgA correlates with protection against RSV infection [21], and antigen-specific serum IgA can be a predictor for secretory IgA (sIgA) in the nasal mucosa [32]. We observed significant antigen-specific serum IgA in NanoSTING-sc9-10 (mean endpoint titer: $4 \pm 1 \times 10^4$) and NanoSTING-SCTM ($4 \pm 1 \times 10^3$) vaccinated mice compared to unvaccinated animals (p-value = 0.004) on day 48 (Fig. 2C). To directly assay mucosal IgA, we tested for prefusion protein-specific IgA in the bronchoalveolar lavage fluid (BALF) and nasal wash samples by ELISA. Both vaccines induce significant IgA titers after the booster dose in the BALF (NanoSTING-sc9-10: $4 \pm 2 \times 10^3$, NanoSTING-SCTM: $3 \pm 2 \times 10^3 \pm$) [Fig. 2D] and nasal wash (NanoSTING-sc9-10: $1 \pm 0.2 \times 10^3$, NanoSTING-SCTM: $1 \pm 0.4 \times 10^3$) [Fig. 2E] compared to PBS-vaccinated mice (BALF: p-value = 0.004, nasal wash: p-value = 0.002).

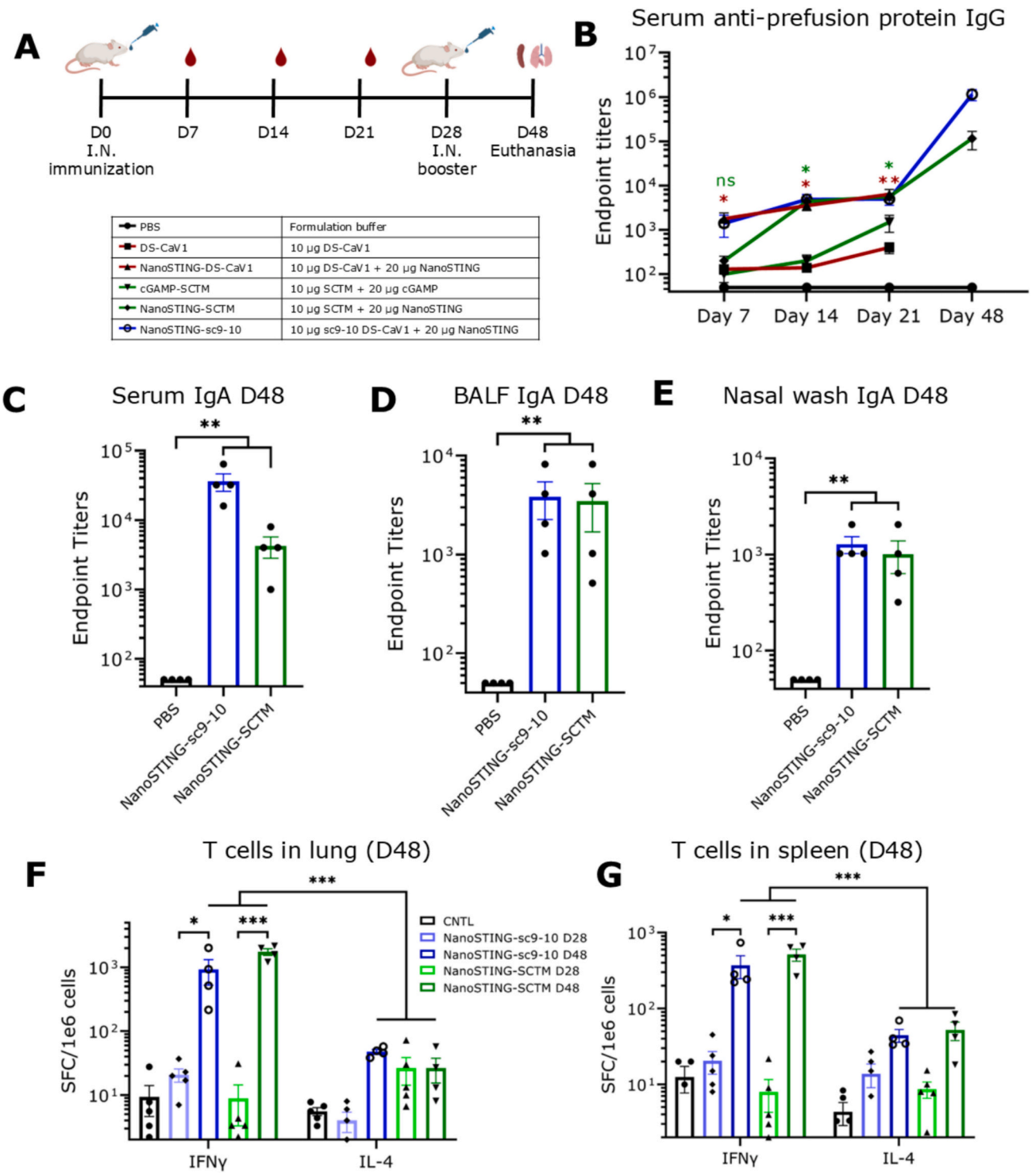

PBS	Formulation buffer
DS-CaV1	10 μg DS-CaV1
NanoSTING-DS-CaV1	10 μg DS-CaV1 + 20 μg NanoSTING
cGAMP-SCTM	10 μg SCTM + 20 μg cGAMP
NanoSTING-SCTM	10 μg SCTM + 20 μg NanoSTING
NanoSTING-sc9-10	10 μg sc9-10 DS-CaV1 + 20 μg NanoSTING

Fig. 2. Intranasal administration of NanoSTING adjuvanted vaccines induces robust humoral and cellular immunity in mice.

A) The intranasal vaccine was formulated by incubating the purified recombinant protein and adjuvant. We immunized six groups (n = 4–5/group) of animals intranasally (IN) with PBS, DS-CaV1, NanoSTING-DS-CaV1, cGAMP-SCTM, NanoSTING-SCTM, and NanoSTING-sc9-10 vaccine formulations. Four weeks after the vaccination, NanoSTING-sc9-10 and NanoSTING-SCTM groups were boosted IN. On day 48, the boosted animals were euthanized to harvest lung and spleen for ELISpot.

B) RSV prefusion protein-specific serum IgG endpoint titers in the vaccinated animals at days 7, 14, 21, and 48. Data are expressed as mean (± SEM) of 4–5 animals. Mann-Whitney t-test p values; ns = $p > 0.05$, *$p < 0.05$,**$p < 0.01$.

C-E) RSV prefusion protein-specific IgA titers in serum (C), BALF (D), and nasal wash (E) on day 48. p values were calculated using the Mann-Whitney t-test (**p < 0.01).

F-G) IFNγ and IL-4 ELISPOT from lung (F) and spleen (G) cells re-stimulated *ex vivo* with RSVB fusion protein peptide pools 20 days after the IN booster dose. Data are expressed as the mean (± SEM) of 4–5 animals assayed. Mann-Whitney t-test p values; *p < 0.05,***$p < 0.001$.

We next evaluated the magnitude of the cellular response by tracking the T cell responses in the spleen (systemic cellular immunity) and the lung (site of disease). Prime-boost immunization with NanoSTING-sc9-10 yielded significantly higher IFNγ secreting T cells in the lung after the second dose [900 ± 400 spot-forming cells (SFC), day 48] in comparison to the primary dose (21 ± 5 SFC, day 28) [*p*-value = 0.0003, Fig. 2F]. This significant increase in IFNγ secreting T cells was also observed in the spleen after two doses of immunization (370 ± 120 SFC, day 48; *vs.* 20 ± 7, day 28, *p*-value = 0.0003) [Fig. 2G]. Similar significant increases in both the lung-resident (1800 ± 200 SFC, day 48; *vs.* 9 ± 6 SFC, day 28, *p*-value = 0.04) and systemic T cell IFNγ responses (520 ± 90 SFC, day 48; *vs.* 8 ± 4 SFC, day 28. *p*-value = 0.02) were observed with dual dose immunization with the NanoSTING-SCTM vaccine. Importantly, both vaccines elicit significantly higher IFNγ-secreting T cells compared to IL-4 secreting T-cells in the lung (*p*-value = 0.002) and the spleen (*p*-value = 0.002), confirming a Th1-biased T-cell response. Taken together, these data suggest that dual-dose NanoSTING-adjuvanted vaccines induce robust antigen-specific antibodies and a Th1/Tc1 T-cell response in immunized mice, regardless of the antigen used for immunization.

3.3. NanoSTING-adjuvanted vaccines induce neutralizing antibodies in cotton rats and protect against viral challenge

We had confirmed the immunogenicity of NanoSTING-adjuvanted vaccines and wanted to evaluate whether our vaccine formulations could induce neutralizing antibodies and protect against viral challenge. We conducted these studies in the standard RSV vaccine preclinical model, cotton rats (*Sigmodon hispidus*), since they are more susceptible to viral infection compared to Balb/c mice [33–35]. We immunized groups of cotton rats intranasally with 1) PBS, 2) NanoSTING-sc9-10, and 3) NanoSTING-SCTM. The animals were boosted with an intranasal dose four weeks after the prime dose (Fig. 3A). We collected serum samples three weeks after the booster dose to evaluate antigen-specific immune responses. RSV prefusion protein-specific ELISAs indicated high serum IgG (NanoSTING-sc9-10: $18 \pm 6 \times 10^4$, NanoSTING-SCTM: $7 \pm 2 \times 10^4$) (Fig. 3B) and IgA (NanoSTING-sc9-10: $2 \pm 0.7 \times 10^3$, NanoSTING-SCTM: $1.5 \pm 0.4 \times 10^3$) (Fig. 3C) titers in vaccinated groups compared to the PBS-administered group (PBS IgG: 100, *p*-value = 0.0001; PBS IgA: 100, *p*-value = 0.0001).

Our experimental vaccines show high serum antibody titers against RSV fusion protein. However, neutralizing antibody titers are a better correlate of protection, as not all binding antibodies can neutralize viral infection [36]. So, we tested the serum collected from the cotton rats on

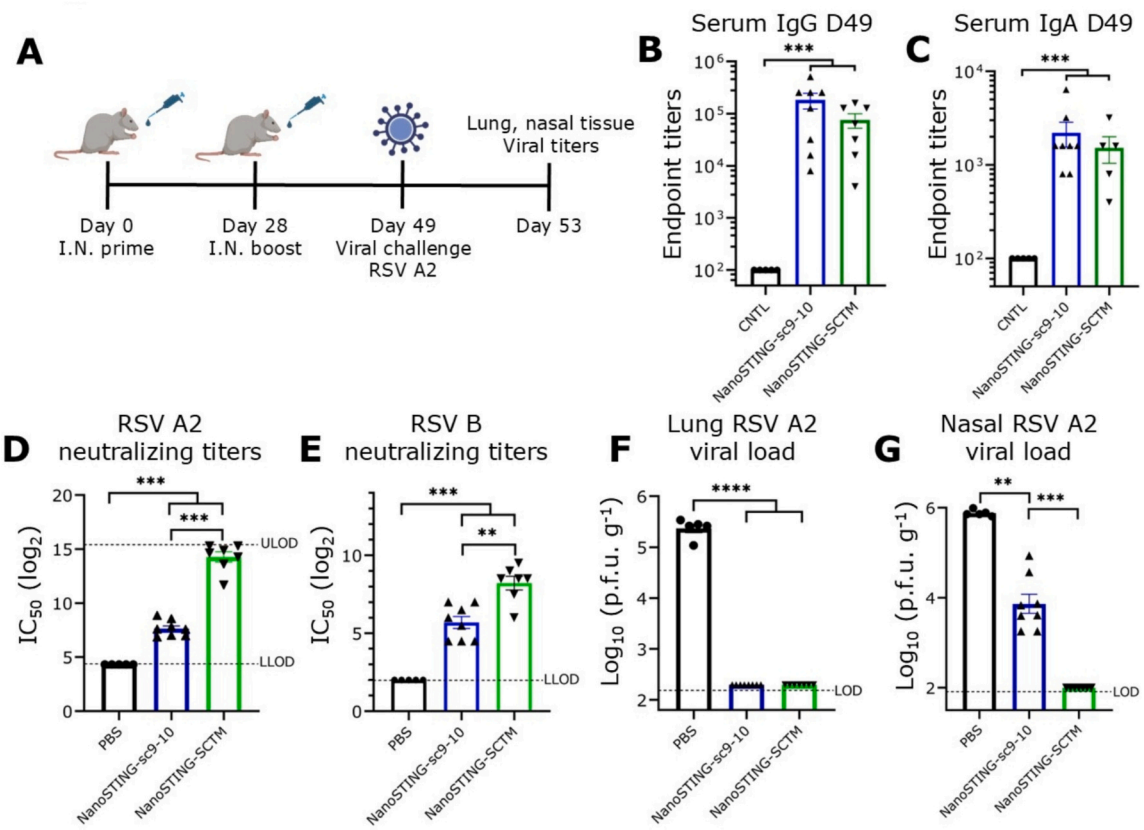

Fig. 3. NanoSTING-adjuvanted vaccines induce virus-neutralizing antibodies in cotton rats and attenuate viral replication in the lung and nasal tissue.
A) We immunized 7–8 female cotton rats IN four weeks apart following a prime-boost vaccination regimen. Vaccinated cotton rats were challenged with 10^5 p.f.u. of RSV A2 at day 48. We also had a group of five cotton rats previously infected with RSV A2 as a positive control. Four days after the challenge, all animals were euthanized to collect lung and nasal tissues for measurement of viral loads.
B–C) RSV prefusion protein-specific serum IgG (B) and IgA (C) titers in vaccinated cotton rats three weeks post-booster dose. Mann-Whitney t-test p value; ***p < 0.001.
D) RSV A2 virus neutralization titers in serum collected (day 48) from vaccinated cotton rats. The limit of detection is shown as a dotted line in the figure. Mann-Whitney t-test p values; *p < 0.05, ***p < 0.001.
E) RSV B virus neutralization titers in serum collected (day 48) from vaccinated cotton rats. The limit of detection is shown as a dotted line in the figure. Mann-Whitney t-test p value; ***p < 0.001.
F–G) RSV virus load in the lung (F) and nasal (G) homogenates collected from challenged cotton rats four days after the viral challenge. Mann-Whitney t-test p values; **p < 0.01, ****p < 0.0001.

day 49 in virus neutralization assays against both strains of RSV (A and B). Both NanoSTING-sc9-10 and NanoSTING-SCTM induce neutralizing antibodies; however, neutralizing titers were significantly higher (p-value = 0.003) for NanoSTING-SCTM (RSV-A2, mean reciprocal of highest dilution $2.5 \pm 0.5 \times 10^4$) compared to NanoSTING-sc9-10 (RSV-A2, $2 \pm 0.4 \times 10^2$) (Fig. 3D). The higher titers were also observed with RSV-B [NanoSTING-SCTM ($4 \pm 1 \times 10^2$) compared to NanoSTING-sc9-10 ($6 \pm 2 \times 10^1$), p-value = 0.0025]. Thus, while immunogenicity studies (serum or BALF IgG, mucosal IgA or lung Th1/Tc1 responses) showed no difference between NanoSTING-sc9-10 and NanoSTING-SCTM, viral neutralization tests demonstrated that NanoSTING-SCTM yielded superior responses compared to NanoSTING-sc9-10 (Fig. 3D).

To verify the efficacy of our experimental vaccines *in vivo,* we challenged the cotton rats with 10^5 plaque-forming units (p.f.u.) RSV A2 virus three weeks after the booster dose. We harvested the lung and nasal tissues four days post-challenge to evaluate viral load at the lower and upper respiratory tract of the cotton rats. Despite a > 100-fold difference in neutralizing antibody titers (Fig. 3D) both NanoSTING-sc9-10 and NanoSTING-SCTM vaccines completely inhibit viral replication in the lung of vaccinated animals (Fig. 3F). Quantification of the viral titers in the nasal compartment upon vaccination yielded surprising results. While NanoSTING-sc9-10 immunization attenuated viral replication in the nasal compartment (viral load- NanoSTING-sc9-10: $2 \pm 1 \times 10^4$, PBS: $8 \pm 1 \times 10^5$, p-value = 0.002), immunization with NanoSTING-SCTM completely eliminated viral replication (Fig. 3G). These results indicate that NanoSTING adjuvanted vaccines induce robust immunity in vaccinated cotton rats that protect against viral challenge.

Recent studies have identified cross-protective monoclonal antibodies that bind to RSV and human metapneumovirus (hMPV) fusion proteins and neutralize them both [37–39]. Despite having only ~35 % amino acid residue identity, the structural similarity of RSV and hMPV prefusion proteins gives rise to cross-protective epitopes (Supplementary Fig. 4A-B) [40,41]. As we utilize the RSV prefusion protein as an immunogen in our studies, we wanted to test the cross-neutralizing potential of these vaccines against hMPV. In this regard, we tested the day 49 serum collected from cotton rats for antibodies against hMPV prefusion protein. We observed that both NanoSTING-sc9-10 (mean endpoint titer, NanoSTING-sc9-10: $3 \pm 1 \times 10^5$, PBS 50) and NanoSTING-SCTM ($4 \pm 2 \times 10^4$) induce high levels of hMPV prefusion protein cross-reactive antibodies (Supplementary Fig. 4C). We also conducted hMPV neutralization assays using day 49 serum from NanoSTING-sc9-10 and NanoSTING-SCTM vaccinated cotton rats. Despite high binding titers, we noted that cross-reactive antibodies elicited by these vaccines could not neutralize the hMPV virus *in vitro* (Supplementary Fig. 4D).

4. Discussion

Following over 60 years of global research efforts, Abrysvo (Pfizer), Arexvy (GSK) and mRESVIA (Moderna) were recently approved for use in adults aged 60 years or older [42,43]. Abrysvo and Arexvy are based on the RSV prefusion protein immunogens, which are well-known for their ability to elicit neutralizing antibodies against the Φ epitope [44]. While Arexvy is formulated by mixing RSV prefusion protein with an AS01E adjuvant, Abrysvo is a bivalent combination of RSV A and RSV B prefusion proteins without an adjuvant [42]. A phase 3 clinical trial reported vaccine efficacy of 85.7 % for Abrysvo against RSV-associated lower respiratory tract (LRT) illness with at least three symptoms [44]. Arexvy was reported to have an efficacy of 83 % against RSV-related LRT disease over a period of 6.7 months [45]. Follow-up phase 3 studies concluded that Abrysvo's efficacy against LRT illness with at least three symptoms in older adults dropped to 77.8 % over two seasons [44]. At the same time, Arexvy's efficacy against RSV-related LRT disease over two seasons dropped to 67.2 % [46]. In contrast to the protein subunit vaccines, mRESVIA is an mRNA vaccine that encodes for the prefusion F protein [47]. The latest of the three approved vaccines, mRESVIA, demonstrated a vaccine efficacy of 82.4 % against RSV-associated LRT disease with at least three symptoms in a phase 2–3 trial conducted across 22 countries [48]. A recent test-negative design analysis found vaccination efficacy against RSV-associated hospitalizations to be 73 % in immunocompromised, and 80 % in adults without any immunocompromising conditions [49].

These approved vaccines and other similar vaccines in phase 3 clinical trials are all administered through the parenteral route [50]. However, as RSV enters the body through the eyes, nose, or mouth, vaccination through the mucosal route can elicit mucosal immunity that protects at the viral port of entry. Not surprising, the current vaccines have not been evaluated on their ability to stop or reduce viral transmission from one infected individual to another. Considering the current scenario, newer vaccination strategies are required to realize the full potential of RSV vaccines against disease and transmission.

Recently, stimulator of interferon gene (STING)-agonists like 2′-3′ cyclic GMP–AMP (cGAMP) have emerged as promising adjuvants that can enhance the mucosal immune response of protein-based vaccines against respiratory pathogens [9,26,51]. cGAMP activates the cGAS/STING cytosolic DNA sensing pathway that results in the secretion of immunostimulatory type-I and type-III interferons [52].

In this study, we formulated RSV prefusion protein-based intranasal vaccines that utilize cGAMP-encapsulating nanoparticles (NanoSTING) as an adjuvant. NanoSTING is a lipid-based adjuvant that protects cGAMP from rapid extracellular degradation and enhances its half-life *in vivo* [53,54]. Additionally, NanoSTING facilitates the decoration of multiple copies of protein antigens on the nanoparticle surface, leading to enhanced immunogenicity and multi-factorial protection against respiratory viruses [26,55]. We tested these vaccines in the cotton rat model, as lung pathology in cotton rats mimics that of humans after RSV infection [56,57]. Both sc9-10 DS-CaV1 and SCTM-based vaccines exhibit neutralizing antibody (nAb) titers against RSV in virus neutralization assays; however, NanoSTING-SCTM induces higher nAb titers than NanoSTING-sc9-10 against both virus subtypes (RSV A and RSV B) (Fig. 3D-E). Lee et al. compared the antibody responses by sc9-10 DS-CaV1 and SCTM-based parenteral vaccines in mice. They reported that following two doses of 10 μg protein administered with AddaVax adjuvant intradermally, sc9-10 DS-CaV1 elicits higher neutralizing antibody titers than SCTM [58]. The contrast between our findings and those of Lee et al. suggests that despite using the same antigens, the route of administration and the adjuvant play critical roles in determining the quality and quantity of the immune response.

We challenged the vaccinated cotton rats with live RSV A2 virus and evaluated viral titers in the lung and nasal tissue. NanoSTING-SCTM eliminates RSV below the limit of detection in both the upper (nose) and lower (lung) respiratory tract (Fig. 3F-G). NanoSTING-sc9-10 fully protected the lung and only partially protected the nose against viral replication (Fig. 3F-G). The difference in protection at the upper respiratory tract between the vaccines may result from the higher neutralization titers elicited by NanoSTING-SCTM. However, serum nAb titers, while necessary, are not a singular correlate of protection against infection [59]. Antigen-specific binding antibodies [60,61], T-cells [62,63], and mucosal immunity (IgA and T-cells) [64,65] are known to complement the protective effects of neutralizing antibodies. NanoSTING adjuvanted vaccines produce similar serum IgG and IgA responses in mice (Fig. 2B-C) and cotton rats (Fig. 3B-C). T-cell responses (Fig. 2F-G) and mucosal immune correlates (BALF and nasal wash IgA) from mice (Fig. 2D-E) further highlight the comparable immunogenicity of both sc9-10 DS-CaV1 and SCTM-based vaccines. Similar immunogenicity profiles and yet variations in nAb titers leading to differential protection observed at the upper respiratory tract may be linked to the inherent stability of the antigen in the vaccine formulation. NanoSTING facilitates the adsorption of proteins on the nanoparticle surface [26], increasing their retention time in the nasal mucosa and promoting uptake by antigen-presenting cells [66]. The physiochemical properties that lead to the adsorption of proteins on nanoparticles can impact the

stability of antigens in vaccine formulation [67,68]. It is possible that adsorption onto NanoSTING stabilizes the SCTM antigen better than the sc9-10 DS-Cav1 antigen. While the SEC-MALS data suggests differences in the stability of the SCTM and sc9-10 DS-CaV1 proteins (Supplementary Fig. 1B), a more thorough investigation into the stability of these antigens in the context of NanoSTING needs to be undertaken.

Due to past cases of vaccine-induced enhanced disease (VED), safety is a major concern in RSV vaccine development. In a clinical trial in the 1960s, a vaccine formulated with formalin-inactivated RSV (FI-RSV) did not elicit protection against natural infections and led to increased disease severity among children vaccinated with FI-RSV compared to children who were not vaccinated [69]. Later, it was discovered that the immune response induced by FI-RSV vaccine is Th2-skewed, and the antibodies induced by the vaccine have low neutralization potential, causing immune-complex formation in the mucosa [70,71]. Our data indicates that NanoSTING adjuvanted prefusion protein vaccines elicit a Th1-skewed response in the lung and spleen of vaccinated animals (Fig. 2F-G), confirming the safety of vaccine-induced immunity.

There is no established animal model to test whether vaccination can prevent transmission of RSV from infected animals to uninfected ones. Chan et al. have demonstrated that RSV-infected ferrets can transmit viruses to cohoused naïve ferrets. However, infected ferrets did not show any sign of weight loss [72]. In the future, it would be interesting to test the efficacy of a NanoSTING-adjuvanted vaccine against viral dissemination in a transmission-permissive animal model.

In summary, we have demonstrated the immunogenic and protective efficacy of NanoSTING as an adjuvant for intranasal vaccine against RSV. Our study highlights the potential of NanoSTING to boost both mucosal and cellular immune responses, offering a promising approach for developing intranasal vaccines against RSV, with possible implications in preventing viral transmission.

CRediT authorship contribution statement

K.M. Samiur Rahman Sefat: Writing – review & editing, Writing – original draft, Visualization, Validation, Project administration, Methodology, Investigation, Formal analysis, Data curation, Conceptualization. **Rohan Kulkarni:** Formal analysis, Data curation. **Jason Trinh:** Formal analysis, Data curation. **Ankita Leekha:** Formal analysis, Data curation. **Monish Kumar:** Formal analysis, Data curation. **Haoran Wu:** Formal analysis, Data curation. **Trevor McBride:** Formal analysis, Data curation. **Letisha Aideyan:** Formal analysis, Data curation. **Vasanthi Avadhanula:** Formal analysis, Data curation. **Pedro A. Piedra:** Supervision, Project administration, Formal analysis. **Stacey M. Louie:** Supervision, Project administration, Formal analysis, Data curation. **Navin Varadarajan:** Writing – review & editing, Supervision, Resources, Project administration, Funding acquisition, Conceptualization.

Declaration of competing interest

The authors declare the following financial interests/personal relationships which may be considered as potential competing interests: Navin Varadarajan reports financial support was provided by National Institutes of Health. Navin Varadarajan reports financial support was provided by AuraVax Therapeutics. Navin Varadarajan reports a relationship with AuraVax Therapeutics and CellChorus that includes: equity or stocks.

Acknowledgments

This publication was supported by the NIH (R01GM143243) and AuraVax Therapeutics.

Appendix A. Supplementary data

Supplementary data to this article can be found online at https://doi.org/10.1016/j.vaccine.2025.127183.

Data availability

Data will be made available on request.

References

[1] Demont C, et al. Economic and disease burden of RSV-associated hospitalizations in young children in France, from 2010 through 2018. BMC Infect Dis Aug. 2021;21(1):730. https://doi.org/10.1186/s12879-021-06399-8.
[2] Lozano R, et al. Global and regional mortality from 235 causes of death for 20 age groups in 1990 and 2010: a systematic analysis for the global burden of disease study 2010. Lancet Dec. 2012;380(9859):2095–128. https://doi.org/10.1016/S0140-6736(12)61728-0.
[3] Glezen WP, Taber LH, Frank AL, Kasel JA. Risk of primary infection and reinfection with respiratory syncytial virus. Am J Dis Child Jun. 1986;140(6):543–6. https://doi.org/10.1001/archpedi.1986.02140200053026.
[4] Li Y, et al. Global, regional, and national disease burden estimates of acute lower respiratory infections due to respiratory syncytial virus in children younger than 5 years in 2019: a systematic analysis. Lancet May 2022;399(10340):2047–64. https://doi.org/10.1016/S0140-6736(22)00478-0.
[5] Falsey AR, Hennessey PA, Formica MA, Cox C, Walsh EE. Respiratory syncytial virus infection in elderly and high-risk adults. N Engl J Med Apr. 2005;352(17):1749–59. https://doi.org/10.1056/NEJMoa043951.
[6] Bukreyev A, Whitehead SS, Murphy BR, Collins PL. Recombinant respiratory syncytial virus from which the entire SH gene has been deleted grows efficiently in cell culture and exhibits site-specific attenuation in the respiratory tract of the mouse. J Virol Dec. 1997;71(12):8973–82. https://doi.org/10.1128/jvi.71.12.8973-8982.1997.
[7] Karron RA, et al. Respiratory syncytial virus (RSV) SH and G proteins are not essential for viral replication in vitro: clinical evaluation and molecular characterization of a cold-passaged, attenuated RSV subgroup B mutant. Proc Natl Acad Sci Dec. 1997;94(25):13961–6. https://doi.org/10.1073/pnas.94.25.13961.
[8] Triantafilou K, Kar S, Vakakis E, Kotecha S, Triantafilou M. Human respiratory syncytial virus viroporin SH: a viral recognition pathway used by the host to signal inflammasome activation. Thorax Jan. 2013;68(1):66–75. https://doi.org/10.1136/thoraxjnl-2012-202182.
[9] Umemoto S, et al. Cationic-nanogel nasal vaccine containing the ectodomain of RSV-small hydrophobic protein induces protective immunity in rodents. npj Vaccines Jul. 2023;8(1):1–16. https://doi.org/10.1038/s41541-023-00700-3.
[10] Schepens B, et al. Protection and mechanism of action of a novel human respiratory syncytial virus vaccine candidate based on the extracellular domain of small hydrophobic protein. EMBO Mol Med Nov. 2014;6(11):1436–54. https://doi.org/10.15252/emmm.201404005.
[11] McLellan JS, Ray WC, Peeples ME. Structure and function of RSV surface glycoproteins. Curr Top Microbiol Immunol 2013;372:83–104. https://doi.org/10.1007/978-3-642-38919-1_4.
[12] Gruber C, Levine S. Respiratory syncytial virus polypeptides. III. The envelope-associated proteins. J Gen Virol 1983;64(4):825–32. https://doi.org/10.1099/0022-1317-64-4-825.
[13] Bolt G, Pedersen LØ, Birkeslund HH. Cleavage of the respiratory syncytial virus fusion protein is required for its surface expression: role of furin. Virus Res Jun. 2000;68(1):25–33. https://doi.org/10.1016/S0168-1702(00)00149-0.
[14] McLellan JS. Neutralizing epitopes on the respiratory syncytial virus fusion glycoprotein. Curr Opin Virol Apr. 2015;11:70–5. https://doi.org/10.1016/j.coviro.2015.03.002.
[15] McLellan JS, et al. Structure of RSV fusion glycoprotein trimer bound to a Prefusion-specific neutralizing antibody. Science May 2013. https://doi.org/10.1126/science.1234914.
[16] Beaumont T, Bakker AQ, Yasuda E. RSV specific binding molecule. US9283274B2. [Online]. Available: https://patents.google.com/patent/US9283274B2/en. [Accessed 22 March 2025].
[17] Tian D, et al. Structural basis of respiratory syncytial virus subtype-dependent neutralization by an antibody targeting the fusion glycoprotein. Nat Commun Nov. 2017;8(1):1877. https://doi.org/10.1038/s41467-017-01858-w.
[18] McLellan JS, et al. Structure-based design of a fusion glycoprotein vaccine for respiratory syncytial virus. Science Nov. 2013;342(6158):592–8. https://doi.org/10.1126/science.1243283.
[19] Joyce MG, et al. Iterative structure-based improvement of a fusion-glycoprotein vaccine against RSV. Nat Struct Mol Biol Sep. 2016;23(9):811–20. https://doi.org/10.1038/nsmb.3267.
[20] Krarup A, et al. A highly stable prefusion RSV F vaccine derived from structural analysis of the fusion mechanism. Nat Commun Sep. 2015;6:8143. https://doi.org/10.1038/ncomms9143.
[21] Habibi MS, et al. Impaired antibody-mediated protection and defective IgA B-cell memory in experimental infection of adults with respiratory syncytial virus. Am J Respir Crit Care Med May 2015;191(9):1040–9. https://doi.org/10.1164/rccm.201412-2256OC.
[22] Van Royen T, Rossey I, Sedeyn K, Schepens B, Saelens X. How RSV proteins join forces to overcome the host innate immune response. Viruses Feb. 2022;14(2):2. https://doi.org/10.3390/v14020419.

[23] Walsh EE, Falsey AR. Humoral and mucosal immunity in protection from natural respiratory syncytial virus infection in adults. J Infect Dis Jul. 2004;190(2):373–8. https://doi.org/10.1086/421524.

[24] Maier C, et al. Mucosal immunization with an adenoviral vector vaccine confers superior protection against RSV compared to natural immunity. Front Immunol Jul. 2022;13. https://doi.org/10.3389/fimmu.2022.920256.

[25] Walker JM, editor. The proteomics protocols handbook. Totowa, NJ: Humana Press; 2005. https://doi.org/10.1385/1592598900.

[26] An X, et al. Single-dose intranasal vaccination elicits systemic and mucosal immunity against SARS-CoV-2. iScience Sep. 2021;24(9):103037. https://doi.org/10.1016/j.isci.2021.103037.

[27] An antigenic analysis of respiratory syncytial virus isolates by a plaque reduction neutralization test - PubMed [Online]. Available: https://pubmed.ncbi.nlm.nih.gov/5933417/. [Accessed 20 December 2024].

[28] Blunck BN, et al. A prospective surveillance study on the kinetics of the humoral immune response to the respiratory syncytial virus fusion protein in adults in Houston, Texas. Vaccine Feb. 2021;39(8):1248–56. https://doi.org/10.1016/j.vaccine.2021.01.045.

[29] Gilman MSA, et al. Characterization of a Prefusion-specific antibody that recognizes a quaternary, cleavage-dependent epitope on the RSV fusion glycoprotein. PLoS Pathog Jul. 2015;11(7):e1005035. https://doi.org/10.1371/journal.ppat.1005035.

[30] Castilow EM, Olson MR, Varga SM. Understanding respiratory syncytial virus (RSV) vaccine-enhanced disease. Immunol Res Nov. 2007;39(1):225–39. https://doi.org/10.1007/s12026-007-0071-6.

[31] Boelen A, et al. Both immunisation with a formalin-inactivated respiratory syncytial virus (RSV) vaccine and a mock antigen vaccine induce severe lung pathology and a Th2 cytokine profile in RSV-challenged mice. Vaccine Nov. 2000;19(7):982–91. https://doi.org/10.1016/S0264-410X(00)00213-9.

[32] Externest D, Meckelein B, Schmidt MA, Frey A. Correlations between antibody immune responses at different mucosal effector sites are controlled by antigen type and dosage. Infect Immun Jul. 2000;68(7):3830–9.

[33] Prince GA, Jenson AB, Horswood RL, Camargo E, Chanock RM. The pathogenesis of respiratory syncytial virus infection in cotton rats. Am J Pathol Dec. 1978;93(3):771–91.

[34] Niewiesk S, Prince G. Diversifying animal models: the use of hispid cotton rats (Sigmodon hispidus) in infectious diseases. Lab Anim Oct. 2002;36(4):357–72. https://doi.org/10.1258/002367702320389026.

[35] Boukhvalova MS, Blanco JCG. The cotton rat Sigmodon hispidus model of respiratory syncytial virus infection. Curr Top Microbiol Immunol 2013;372:347–58. https://doi.org/10.1007/978-3-642-38919-1_17.

[36] McCool RS, et al. Vaccination with prefusion-stabilized respiratory syncytial virus fusion protein elicits antibodies targeting a membrane-proximal epitope. J Virol Sep. 2023;97(10). https://doi.org/10.1128/jvi.00929-23. e00929–23.

[37] Corti D, et al. Cross-neutralization of four paramyxoviruses by a human monoclonal antibody. Nature Sep. 2013;501(7467):439–43. https://doi.org/10.1038/nature12442.

[38] Schuster JE, et al. A broadly neutralizing human monoclonal antibody exhibits in vivo efficacy against both human Metapneumovirus and respiratory syncytial virus. J Infect Dis Jan. 2015;211(2):216–25. https://doi.org/10.1093/infdis/jiu307.

[39] Wen X, et al. Potent cross-neutralization of respiratory syncytial virus and human metapneumovirus through a structurally conserved antibody recognition mode. Cell Host Microbe Aug. 2023;31(8). https://doi.org/10.1016/j.chom.2023.07.002. 1288–1300.e6.

[40] Madeira F, et al. The EMBL-EBI job dispatcher sequence analysis tools framework in 2024. Nucleic Acids Res Jul. 2024;52(W1):W521–5. https://doi.org/10.1093/nar/gkae241.

[41] Robert X, Gouet P. Deciphering key features in protein structures with the new ENDscript server. Nucleic Acids Res Jul. 2014;42(W1):W320–4. https://doi.org/10.1093/nar/gku316.

[42] Venkatesan P. First RSV vaccine approvals. The Lancet Microbe Aug. 2023;4(8):e577. https://doi.org/10.1016/S2666-5247(23)00195-7.

[43] Moderna receives U.S. FDA approval for RSV vaccine mRESVIA(R) [Online]. Available: https://investors.modernatx.com/news/news-details/2024/Moderna-Receives-U.S.-FDA-Approval-for-RSV-Vaccine-mRESVIAR/default.aspx. [Accessed 8 March 2025].

[44] Pfizer. A phase 3 study to evaluate the efficacy, immunogenicity, and safety of respiratory syncytial virus (RSV) Prefusion F subunit vaccine in adults. clinicaltrials.gov, Clinical trial registration NCT05035212. [Online]. Available: https://clinicaltrials.gov/study/NCT05035212. [Accessed 31 December 2023].

[45] GlaxoSmithKline. A Phase 3, Randomized, Placebo-controlled, Observer-blind, Multi-country Study to Demonstrate the Efficacy of a Single Dose and Annual Revaccination Doses of GSK's RSVPreF3 OA Investigational Vaccine in Adults Aged 60 Years and Above. clinicaltrials.gov, Clinical trial registration NCT04886596. [Online]. Available: https://clinicaltrials.gov/study/NCT04886596. [Accessed 31 December 2023].

[46] Ison MG, et al. Efficacy and Safety of Respiratory Syncytial Virus (RSV) Prefusion F Protein Vaccine (RSVPreF3 OA) in Older Adults Over 2 RSV Seasons. Clin Infect Dis Jan. 2024. https://doi.org/10.1093/cid/ciae010. p. ciae010.

[47] Biscaia-Caleiras M, Fonseca NA, Lourenço AS, Moreira JN, Simões S. Rational formulation and industrial manufacturing of lipid-based complex injectables: landmarks and trends. J Control Release Sep. 2024;373:617–39. https://doi.org/10.1016/j.jconrel.2024.07.021.

[48] Wilson E, et al. Efficacy and safety of an mRNA-based RSV PreF vaccine in older adults. N Engl J Med Dec. 2023;389(24):2233–44. https://doi.org/10.1056/NEJMoa2307079.

[49] Payne AB, et al. Respiratory syncytial virus (RSV) vaccine effectiveness against RSV-associated hospitalisations and emergency department encounters among adults aged 60 years and older in the USA, October, 2023, to March, 2024: a test-negative design analysis. Lancet Oct. 2024;404(10462):1547–59. https://doi.org/10.1016/S0140-6736(24)01738-0.

[50] Ruckwardt TJ. The road to approved vaccines for respiratory syncytial virus. npj Vaccines Sep. 2023;8(1):1–8. https://doi.org/10.1038/s41541-023-00734-7.

[51] Xiao L, Yu W, Shen L, Yan W, Qi J, Hu T. Mucosal SARS-CoV-2 nanoparticle vaccine based on mucosal adjuvants and its immune effectiveness by intranasal administration. ACS Appl Mater Interfaces Aug. 2023;15(30):35895–905. https://doi.org/10.1021/acsami.3c05456.

[52] Wu J, et al. Cyclic GMP-AMP is an endogenous second messenger in innate immune signaling by cytosolic DNA. Science Feb. 2013;339(6121):826–30. https://doi.org/10.1126/science.1229963.

[53] Li L, et al. Hydrolysis of 2′3′-cGAMP by ENPP1 and design of non-hydrolyzable analogs. Nat Chem Biol Dec. 2014;10(12):1043–8. https://doi.org/10.1038/nchembio.1661.

[54] Wehbe M, et al. Nanoparticle delivery improves the pharmacokinetic properties of cyclic dinucleotide STING agonists to open a therapeutic window for intravenous administration. J Control Release Feb. 2021;330:1118–29. https://doi.org/10.1016/j.jconrel.2020.11.017.

[55] Leekha A, et al. An intranasal nanoparticle STING agonist has broad protective immunity against respiratory viruses and variants. bioRxiv Apr. 19, 2022. https://doi.org/10.1101/2022.04.18.488695.

[56] Boukhvalova MS, Prince GA, Blanco JCG. The cotton rat model of respiratory viral infections. Biologicals Jun. 2009;37(3):152–9. https://doi.org/10.1016/j.biologicals.2009.02.017.

[57] Fuentes S, Coyle EM, Golding H, Khurana S. Nonglycosylated G-protein vaccine protects against homologous and heterologous respiratory syncytial virus (RSV) challenge, while glycosylated G enhances RSV lung pathology and cytokine levels. J Virol Jul. 2015;89(16):8193–205. https://doi.org/10.1128/jvi.00133-15.

[58] Lee Y-Z, et al. A tale of two fusion proteins: understanding the metastability of human respiratory syncytial virus and metapneumovirus and implications for rational design of uncleaved prefusion-closed trimers. bioRxiv Mar. 2024:583986. https://doi.org/10.1101/2024.03.07.583986.

[59] Sun K, et al. SARS-CoV-2 correlates of protection from infection against variants of concern. Nat Med Oct. 2024;30(10):2805–12. https://doi.org/10.1038/s41591-024-03131-2.

[60] Favresse J, et al. Vaccine-induced binding and neutralizing antibodies against omicron 6 months after a homologous BNT162b2 booster. J Med Virol 2023;95(1):e28164. https://doi.org/10.1002/jmv.28164.

[61] Edara VV, et al. Infection- and vaccine-induced antibody binding and neutralization of the B.1.351 SARS-CoV-2 variant. Cell Host Microbe Apr. 2021;29(4):516–521.e3. https://doi.org/10.1016/j.chom.2021.03.009.

[62] Antoun E, Peng Y, Dong T. Vaccine-induced CD8+ T cells are key to protection from SARS-CoV-2. Nat Immunol Oct. 2023;24(10):1594–6. https://doi.org/10.1038/s41590-023-01621-y.

[63] Sheetikov SA, et al. Clonal structure and the specificity of vaccine-induced T cell response to SARS-CoV-2 spike protein. Front Immunol Apr. 2024;15. https://doi.org/10.3389/fimmu.2024.1369436.

[64] Holmgren J, Czerkinsky C. Mucosal immunity and vaccines. Nat Med Apr. 2005;11(4 Suppl):S45–53. https://doi.org/10.1038/nm1213.

[65] Alqahtani SAM. Mucosal immunity in COVID-19: a comprehensive review. Front Immunol Aug. 2024;15. https://doi.org/10.3389/fimmu.2024.1433452.

[66] Sefat KMSR, et al. An intranasal nanoparticle vaccine elicits protective immunity against *mycobacterium tuberculosis*. Vaccine Sep. 2024;42(22):125909. https://doi.org/10.1016/j.vaccine.2024.04.055.

[67] Almeida AJ, Souto E. Solid lipid nanoparticles as a drug delivery system for peptides and proteins. Adv Drug Deliv Rev Jul. 2007;59(6):478–90. https://doi.org/10.1016/j.addr.2007.04.007.

[68] Haynes CA, Norde W. Globular proteins at solid/liquid interfaces. Colloids Surf B: Biointerfaces Jul. 1994;2(6):517–66. https://doi.org/10.1016/0927-7765(94)80066-9.

[69] Kim HW, et al. Respiratory syncytial virus disease in infants despite prior administration of antigenic inactivated vaccine. Am J Epidemiol Apr. 1969;89(4):422–34. https://doi.org/10.1093/oxfordjournals.aje.a120955.

[70] Eichinger KM, et al. Prior respiratory syncytial virus infection reduces vaccine-mediated Th2-skewed immunity, but retains enhanced RSV F-specific CD8 T cell responses elicited by a Th1-skewing vaccine formulation. Front Immunol Oct. 2022;13:1025341. https://doi.org/10.3389/fimmu.2022.1025341.

[71] Knudson CJ, Hartwig SM, Meyerholz DK, Varga SM. RSV vaccine-enhanced disease is orchestrated by the combined actions of distinct CD4 T cell subsets. PLoS Pathog Mar. 2015;11(3):e1004757. https://doi.org/10.1371/journal.ppat.1004757.

[72] Chan KF, et al. Pathogenesis, Humoral Immune Responses, and Transmission between Cohoused Animals in a Ferret Model of Human Respiratory Syncytial Virus Infection. J Virol Jan. 2018;92(4). https://doi.org/10.1128/jvi.01322-17.